Pure Nuclear Quadrupole Spectra of Chlorine and Antimony Isotopes in Solids*

TIEN-CHUAN WANG
Columbia University, New York, New York
(Received March 21, 1955)

Experimental measurements on nuclear quadrupole resonances of chlorine and antimony isotopes in solids have been made to an accuracy of about 0.001 percent. The results are compared in detail with theoretical results for (1) nuclear quadrupole interaction, (2) interaction between quadrupole coupling and thermal vibrations, and (3) effects of a nuclear hexadecapole. The ratio $(eQq)_{Cl^{35}}/(eQq)_{Cl^{37}}$ varies between 1.268736 and 1.268973 while $(eQq)_{Sb^{123}}/(eQq)_{Sb^{121}}$ varies from 1.274714 to 1.274770. These variations may be attributed to zero-point vibrations and to thermal vibrations, so that no clear evidence is found for nuclear polarization by surrounding electric fields. For *p*-dichlorobenzene, the temperature coefficient of the coupling constant of Cl and the variation of isotopic coupling ratio with temperature are shown to be in fair quantitative agreement with the extension of Bayer's theory of vibrational effects. Relaxation times, Zeeman effects, and certain effects due to crystal structure are examined. Small discrepancies in the measured ratios of frequencies of transitions in Sb^{121} and Sb^{123}, which can be attributed to nuclear hexadecapole interactions are found. These indicate a hexadecapole coupling constant in Sb^{123} of 24 kc/sec and a ratio of the Sb^{123} hexadecapole coupling to that of Sb^{121} of 0.8 ± 0.3. A convenient high-sensitivity circuit for observation of nuclear resonances in solids has been developed and is discussed.

I. INTRODUCTION

HYPERFINE structure which arises from the electrical quadrupole interaction between nuclei and their surrounding electrons has been extensively observed in atomic and molecular spectra. The quadrupole coupling constant eQq, which is the main object of these measurements, gives information regarding the distribution of electrons around a nucleus and the deviation of the nucleus from spherical symmetry. This information may, in turn, be utilized to determine molecular[1,2] and nuclear structures and to shed light on solid state phenomena. Because of the inherent difficulty in measuring the small frequency difference associated with the quadrupole hyperfine structure, the value of eQq cannot easily be obtained to high accuracy by using methods of optical or molecular spectroscopy. Experiments on pure nuclear quadrupole resonances yields data of much higher accuracy.[3–5] With the experimental setup of the present experiment, the quadrupole resonance frequencies can be measured to an accuracy of better than 0.001 percent. With this accuracy the ratios of eQq of different isotopes were found to be dependent upon temperature and molecular environment. In order to evaluate these experimental results, it has been necessary to calculate nuclear quadrupole interactions with much greater care than is usual. The effects of several very small interaction terms were included and compared with the experimental data.

* Work supported jointly by the Signal Corps, the Office of Naval Research, and the Air Research and Development Command.

[1] C. H. Townes and B. P. Dailey, J. Chem. Phys. **17**, 782 (1949).
[2] C. H. Townes and B. P. Dailey, J. Chem. Phys. **20**, 35 (1952).
[3] In the preliminary result of the present experiment, the ratio $(eQq)_{Cl^{35}}/(eQq)_{Cl^{37}}$ in solid *trans*-dichloroethylene was found to be 1.2682 ± 0.0004. This was the first accurate value obtained. This ratio was quoted by Geschwind, Gunther-Mohr, and Townes, Phys. Rev. **81**, 288 (1951); but the accuracy stated there involves a typographical error. The probable error should read 0.0004 instead of 0.004.
[4] Wang, Townes, Schawlow, and Holden, Phys. Rev. **86**, 809 (1952).
[5] R. Livingston, Phys. Rev. **82**, 289 (1951).

II. THEORY

A. General Formulation

The electrical interaction between an atomic nucleus and its neighboring electronic charge can be expressed in a series corresponding to the effects of various electrical multipoles. In this series, the first term represents the interaction of a point charge with the electronic field while the second and third terms describe electric quadrupole and hexadecapole (16th-pole) interactions. These last two terms are not zero only if the shape of nucleus and the distribution of its surrounding electrons depart from spherical symmetry. The Hamiltonian operator for the nuclear quadrupole interaction can be written as

$$H_Q=\frac{eQq}{4I(2I-1)}\left[(3I_z^2-I^2)+\tfrac{1}{2}\eta(I_+^2+I_-^2)\right]_{\mathrm{op}}. \quad (1)$$

This representation can be obtained by a simplification of the formulation given by Pound,[6] Bersohn,[7] or Dehmelt and Krüger.[8] Here I represents the spin of the nucleus, $I_\pm\equiv I_x\pm iI_y$, Q is the nuclear quadrupole moment,

$$q\equiv\int_{\tau_e}\frac{\rho(r_e)(3\cos^2\theta_e-1)}{r_e^3}d\tau_e\equiv-\frac{\partial E_z}{\partial z},$$

where r_e and θ_e are polar coordinates of the electronic charge element $\rho d\tau_e$ considered from the center of symmetry, q is the principal value of the field gradient at the nucleus, and

$$\eta\equiv\left(\frac{\partial E_x}{\partial x}-\frac{\partial E_y}{\partial y}\right)\Big/\frac{\partial E_z}{\partial z}$$

is the asymmetry parameter of the field gradient in a plane perpendicular to the z direction. In all cases, $1\geq|\eta|\geq0$. Matrix elements of the operator in Eq. (1)

[6] R. V. Pound, Phys. Rev. **79**, 685 (1950).
[7] R. Bersohn, J. Chem. Phys. **20**, 1505 (1952).
[8] H. G. Dehmelt and H. Krüger, Z. Physik **129**, 401 (1951).

can be derived from well-known matrices for quantum-mechanical angular momentum.[9] In an I, m representation, the first term in Eq. (1) gives diagonal elements which are the main parts of the characteristic energies. The second term represents off-diagonal elements corresponding to $\Delta m=\pm 2$. They are nonvanishing only when the asymmetry-parameter η is different from zero.

B. Energy Levels

The nuclear quadrupole moment is zero unless $I\geqslant 1$. For integral values of I, Eq. (1) will lead to solutions for the energy levels which are similar to those of a molecular asymmetric rotor.[10] In general, for the case of half-integral spin, the $2I+1$ energy levels are doubly degenerate, so that the secular equation of degree $2I+1$ can be factored into two identical equations of degree $I+\frac{1}{2}$. If spin I is greater than $\frac{3}{2}$, it is impossible to obtain the exact solution in closed form. However, the energy levels can be obtained by the use of an approximation method to solve the secular equation.

For I equal to $\frac{3}{2}$, the exact solution[2,11] for the energy level is

$$W_{m=\pm\frac{3}{2}'}=-\tfrac{1}{4}eQq(1+\tfrac{1}{3}\eta^2)^{\frac{1}{2}},$$
$$W_{m=\pm\frac{1}{2}'}=\tfrac{1}{4}eQq(1+\tfrac{1}{3}\eta)^{\frac{1}{2}}, \tag{2}$$

where the primed m indicates those states which are modified by the asymmetry parameter.

For $I=5/2$, the energy levels which are obtained from the expansion in powers[12] of η^2 are

$$W_{\pm\frac{1}{2}'}=\frac{-eQq}{5}\left(1+\frac{4}{9}\eta^2-\frac{172}{729}\eta^4+\frac{15\,332}{59\,049}\eta^6-\frac{1\,717\,580}{4\,782\,969}\eta^8\right), \tag{3a}$$

$$W_{\pm\frac{3}{2}'}=\frac{-eQq}{20}\left(1-\frac{3}{2}\eta^2+\frac{23}{24}\eta^4-\frac{449}{432}\eta^6+\frac{44\,675}{31\,104}\eta^8\right), \tag{3b}$$

$$W_{\pm\frac{5}{2}'}=\frac{eQq}{4}\left(1+\frac{1}{18}\eta^2+\frac{17}{5832}\eta^4-\frac{143}{944\,784}\eta^6-\frac{12\,587}{612\,220\,032}\eta^8\right). \tag{3c}$$

[9] These matrices are:

$$\langle m|I_z|m\rangle=m,$$
$$\langle I,m|I_\pm|I,m\mp1\rangle=[(I\pm m)(I\mp m+1)]^{\frac{1}{2}},$$
$$\langle I,m|I^2|I,m\rangle=I(I+1),$$
$$\langle I,m|I_\pm{}^2|I,m\mp2\rangle=[(I\pm m)(I\pm m-1)(I\mp m+1)(I\mp m+2)]^{\frac{1}{2}}.$$

[10] King, Hainer, and Cross, J. Chem. Phys. **11**, 27 (1943).

[11] Christopher Dean, dissertation, Harvard University, June, 1952 (unpublished).

[12] Bershon (reference 7) has obtained the solutions for $I=5/2$ up to eighth-order terms. However, his sixth order coefficient of η for $W_{m=\frac{5}{2}'}$ differs from the present value. Private communication with him establishes that the fourth term in his Eq. (21a) should read $-(715/472\,392)\eta^6$, which is the same as the present result.

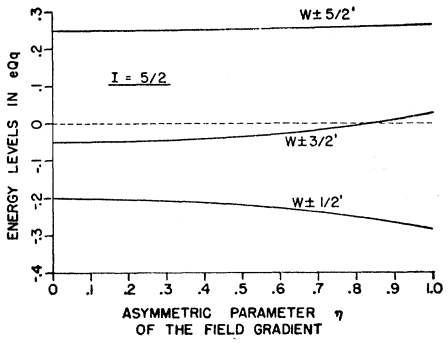

FIG. 1. Energy levels of the quadrupole interaction for $I=5/2$.

Figure 1 shows energy levels as functions of η. If $\eta=0$, the two transitions $\nu_1=W_{\pm\frac{3}{2}'}-W_{\pm\frac{1}{2}'}$, and $\nu_2=W_{\pm\frac{5}{2}'}-W_{\pm\frac{1}{2}'}$, have the simple ratio $\nu_2/\nu_1=2$.

Similarly, for spin $I=7/2$, the energy levels are approximately[13]

$$W_{\pm\frac{1}{2}'}=-\frac{5}{28}eQq\left(1+\frac{5}{6}\eta^2-\frac{311}{216}\eta^4+\frac{20\,557}{3888}\eta^6-\frac{762\,019}{31\,104}\eta^8\right), \tag{4a}$$

$$W_{\pm\frac{3}{2}'}=-\frac{3}{28}eQq\left(1-\frac{31}{30}\eta^2+\frac{21\,967}{9000}\eta^4-\frac{3\,975\,973}{450\,000}\eta^6+\frac{734\,970\,487}{18\,000\,000}\eta^8\right), \tag{4b}$$

$$W_{\pm\frac{5}{2}'}=\frac{eQq}{28}\left(1+\frac{5}{6}\eta^2+\frac{25}{216}\eta^4-\frac{275}{3888}\eta^6-\frac{25}{93\,312}\eta^8\right), \tag{4c}$$

$$W_{\pm\frac{7}{2}'}=\frac{7}{28}eQq\left(1+\frac{1}{30}\eta^2+\frac{29}{27\,000}\eta^4+\frac{1241}{12\,150\,000}\eta^6+\frac{2263}{1\,458\,000\,000}\eta^8\right). \tag{4d}$$

Figure 2 gives the dependence of the energy levels on η. If we take $\nu_1=W_{\pm\frac{3}{2}'}-W_{\pm\frac{1}{2}'}$, $\nu_2=W_{\pm\frac{5}{2}'}-W_{\pm\frac{3}{2}'}$, and $\nu_3=W_{7/2'}-W_{\frac{5}{2}'}$, the ratio of transition frequencies $\nu_3:\nu_2:\nu_1$ should be 3:2:1 for the case $\eta=0$.

C. Effects of Thermal Vibrations

It is well known that the quadrupole coupling constant eQq measured in pure nuclear quadrupole resonances is temperature dependent. Dehmelt, Krüger[8] and later Bayer[14] suggested that this temperature dependence was caused solely by thermal vibrations of molecules in crystals and Dean[11] has studied the effects of thermal vibrations on chlorine resonances in a group

[13] R. Bersohn has kindly checked the results of this calculation.

[14] H. Bayer, Z. Physik **130**, 227 (1951).

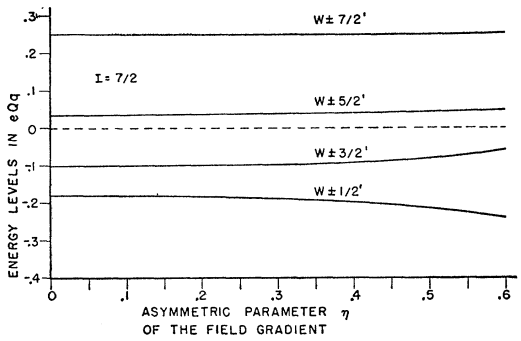

FIG. 2. Energy levels of the quadrupole interaction for $I=7/2$.

of molecular crystals. As molecules execute molecular (torsional) and intramolecular (stretching and bending) oscillations in crystals, the charge distribution in the molecules becomes distorted and the principal axes of the electric field gradient are varied so that a variation[15,16] in q is to be expected. For the sake of illustration one may consider p-dichlorobenzene, a molecular crystal whose principal torsional vibration frequencies have been well identified.[17,18] Since chlorine atoms are bonded to the benzene rings at opposite corners, two modes of thermal vibrations involving rotation around the principal molecular axes perpendicular to the chlorine bonds will be effective in the temperature variation of the q of the chlorine. Because of this effect, the quadrupole Hamiltonian operator becomes

$$H_Q=\frac{eQq'}{4I(2I-1)}[(3I_z^2-I^2)+\tfrac{1}{2}\eta'(I_+^2+I_-^2)]_{\rm op}; \quad (5a)$$

where

$$q'=q[1-\tfrac{3}{2}(\langle\theta^2\rangle_{\rm Av}+\langle\phi^2\rangle_{\rm Av})+\tfrac{1}{2}\eta(\langle\theta^2\rangle_{\rm Av}-\langle\phi^2\rangle_{\rm Av}) +\tfrac{1}{2}(3-\eta)\langle\theta^2\rangle_{\rm Av}\langle\phi^2\rangle_{\rm Av}], \quad (5b)$$

and

$$\eta'=(q/q')[\eta+\tfrac{3}{2}(\langle\theta^2\rangle_{\rm Av}-\langle\phi^2\rangle_{\rm Av})-\tfrac{1}{2}\eta(\langle\theta^2\rangle_{\rm Av}+\langle\phi^2\rangle_{\rm Av}) +\tfrac{1}{2}(3-\eta)\langle\theta^2\rangle_{\rm Av}\langle\phi^2\rangle_{\rm Av}], \quad (5c)$$

express the modifications of q and η due to the thermal vibrations. They are functions of the mean square amplitudes $\langle\phi^2\rangle_{\rm Av}$ and $\langle\theta^2\rangle_{\rm Av}$ of rotation about the two principal axes x and y respectively. According to Bayer's formulation, $\langle\phi^2\rangle_{\rm Av}$ and $\langle\theta^2\rangle_{\rm Av}$ are both functions of the absolute temperature T and of the molecular vibration constants (such as vibration frequencies and moments of inertia around x- and y-axes).

The Hamiltonian operator from Eq. (5a) has exactly the same form as in Eq. (1). The only effect which is caused by thermal vibrations is the change of q to q', and of η to η'. In the case $I=\frac{3}{2}$ which occurs in chlorine nuclei, by neglecting higher order terms in thermal vibration amplitudes, the temperature coefficient for the quadrupole resonance frequency is found to be

$$\frac{1}{\nu_0}\left(\frac{d\nu}{dT}\right)=\frac{-3\hbar^2}{2kT^2}\left[\frac{e^{h\nu_a/kT}}{I_x(e^{h\nu_a/kT}-1)^2}+\frac{e^{h\nu_b/kT}}{I_y(e^{h\nu_b/kT}-1)^2}\right], \quad (6a)$$

where ν_0 is the pure quadrupole resonance frequency for $\eta=0$, I_x and I_y are momenta of inertia of the molecule perpendicular to the bond direction of the chlorines, ν_a and ν_b the corresponding frequencies of torsional vibrations, k=Boltzmann's constant and $\hbar$=Planck's constant divided by 2π. Under ordinary conditions, $h\nu_a/kT$ and $h\nu_b/kT\ll 1$, so that Eq. (6a) becomes

$$\frac{1}{\nu_0}\left(\frac{d\nu}{dT}\right)=-\frac{3k}{8\pi^2}\left[\frac{e^{h\nu_a/kT}}{I_x\nu_a^2}+\frac{e^{h\nu_b/kT}}{I_y\nu_b^2}\right]. \quad (6b)$$

This equation indicates that the magnitude of the temperature coefficient $\nu_0^{-1}(d\nu/dT)$ decreases as the frequency of the torsional vibration increases. Moreover, for the chlorine resonances,[19] the ratio $(eQq)_{35}/(eQq)_{37}$ will be

$$\frac{(eQq)_{\rm Cl^{35}}}{(eQq)_{\rm Cl^{37}}}=\frac{\nu_{35}}{\nu_{37}}=\frac{(eQq)_{35}^0}{(eQq)_{37}^0} \times\left[1-\frac{3\hbar^2}{8I_{x35}kT}\frac{\Delta I_x}{I_{x35}}-\frac{3\hbar^2}{8I_{y35}kT}\frac{\Delta I_y}{I_{y35}}\right], \quad (7)$$

where $\Delta I\equiv I_{37}-I_{35}$, ν_{35} and ν_{37} are the pure quadrupole resonance frequencies of Cl^{35} and Cl^{37}, and $(eQq)^0$ the quadrupole coupling constant when $\eta=0$ and when there are no thermal vibrations. Equation (7) indicates that $(eQq)_{\rm Cl^{35}}/(eQq)_{\rm Cl^{37}}$ decreases with a decrease of temperature T. Since $1/I_{x35}$ and $1/I_{y35}$ are proportional to ν_a^2 and ν_b^2, the squares of the torsional vibration frequencies, the temperature effect on the ratio of quadrupole coupling constants of isotopes as given in Equation (7) is larger for the higher-frequency modes of torsional vibration. Figure 3 shows the deviation $\Delta\nu$ from ν_0 (or Δq from q_0) of the resonance frequencies with temperature (where for simplicity, it is assumed that only one mode is excited). The solid curve represents the dependence of the quadrupole coupling constant (actually q) of Cl^{37} and the dotted one that of Cl^{35}. The two curves coincide at high temperature, and separate at low temperature due to the slightly different effect of thermal vibrations for different isotopes. Since the ratio of quadrupole moments, Q_{35}/Q_{37}, is constant, the ratio $(eQq)_{35}/(eQq)_{37}$, will vary with temperature as does q_{35}/q_{37} shown in Fig. 3, so that it should decrease with decreasing temperature. When the absolute temperature T approaches zero, zero point vibrations are still effective in changing q and give an appreciable difference between q_{35} and q_{37}.

[15] Fabricand, Carlson, Lee, and Rabi, Phys. Rev. **91**, 1403 (1953).
[16] H. J. Zeiger and D. I. Bolef, Phys. Rev. **85**, 788 (1952).
[17] A. Kastler and A. Rousset, Phys. Rev. **71**, 455 (1947).
[18] B. D. Saksena, J. Chem. Phys. **18**, 1653 (1950).

[19] Both Cl^{35} and Cl^{37} possess spins of $\frac{3}{2}$.

D. Hexadecapole Interaction

As mentioned previously, after the quadrupole term the next term to be considered in the interaction of the nucleus with its surrounding electronic charge is the hexadecapole term. This term can be written as

$$H_{\text{hex}}\equiv\int_{\tau_e}\int_{\tau_n}\rho_e{}^e\rho_n\frac{r_n{}^4}{r_e{}^5}P_4(\cos\theta_{en})d\tau_e d\tau_n$$

$$=\int_{\tau_e}\int_{\tau_n}\frac{\rho_e{}^e\rho_n r_n{}^4}{r_e{}^5}(-1)^m Z_4{}^{(m)}(n)Z_4{}^{(-m)}(e)d\tau_e d\tau_n,\qquad r_e>r_n,\quad (8a)$$

where the $Z_4{}^{(m)}$ are defined as

$$Z_4{}^{(m)}=(-1)^m\left[\frac{(l-m)!}{(l+m)!}\right]^{\frac{1}{2}}\sin^m\theta\frac{d^m}{d^m(\cos\theta)}\times P_4(\cos\theta)e^{im\phi},\quad (8b)$$

$$Z_4{}^{(-m)}=(-1)^m Z_4{}^{(m)};$$

and $\cos\theta_{en}=\cos\theta_e\cos\theta_n+\sin\theta_e\sin\theta_n\cos(\phi_e-\phi_n)$. θ_{en} is the angle between the electronic position r_e and the nuclear position r_n referred to the center of symmetry of the molecules, and θ_n, θ_e, ϕ_n, and ϕ_e are the nuclear and the electronic polar and azimuthal angles respectively. One may define the principal hexadecapole field as

$$m_{16}\equiv-\frac{\partial^3 E_z}{\partial z^3}=\int_{\tau_e}\frac{\rho_e{}^e(r_e)(35\cos^4\theta_e-30\cos^2\theta_e+3)d\tau_e}{r_e{}^5},\quad (9a)$$

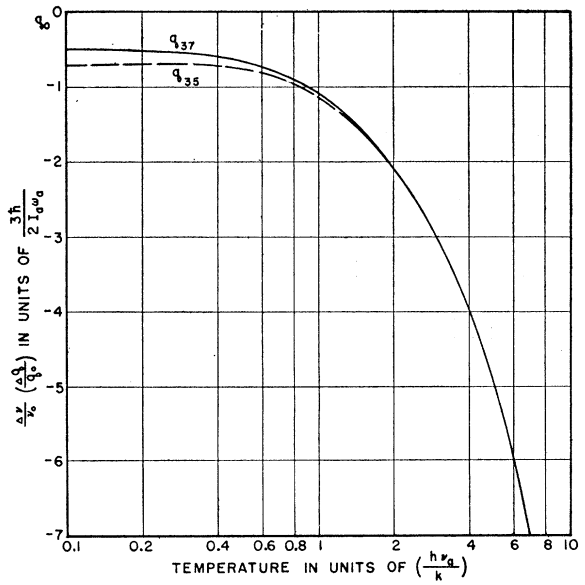

FIG. 3. Dependence of nuclear quadrupole resonance frequencies on temperature. The solid curve is for Cl^{37} and the dotted curve for Cl^{35}.

and

$$eM_{16}\equiv\int_{\tau_n}\psi^*_{I,m=I}r_n{}^4(35\cos^4\theta_n-30\cos^2\theta_n+3)\times\psi_{I,m=I}d\tau_n,\quad (9b)$$

where M_{16} is the nuclear hexadecapole moment, which will be zero unless $I\geqslant 2$. m_{16} is inversely proportional to $r_e{}^5$ and hence decrease more rapidly with an increase of r_e than does the corresponding quantity q for a quadrupole interaction. Expression (9a) vanishes for either an s or p electron, but not for electrons of higher angular momentum. Hence electrons in d and f orbitals will make the most important contribution to m_{16}. The hexadecapole moment M_{16} is a quantity which describes the second order departure of the nuclear charge distribution from spherical symmetry.

Taking only those operators in Eq. (8b) for which $m=0$, and symmetrizing, one obtains the principal quantity in the Hamiltonian for the nuclear hexadecapole interaction,

$$H_{\text{hex}}=\frac{eM_{16}m_{16}}{128I(I-1)(2I-1)(2I-3)}\times[35I_z{}^4-30I_z{}^2I^2+3I^4+25I_z{}^2-6I^2]_{\text{op}}.\quad (10)$$

This equation applies only where $I\geqslant 2$, which is the condition required for existence of a hexadecapole moment. The ratio $eM_{16}m_{16}/eQq$ may be seen to be approximately $r_n{}^2/r_{\text{eff}}{}^2$, where r_n is the nuclear radius and r_{eff} is an average distance of the electron from the nucleus.

For $I=5/2$, the energy levels for the hexadecapole interaction will be, from Eq. (10)

$$\begin{aligned}W(\text{hex})_{m=\pm\frac{1}{2}}&=(3/96)(eM_{16}m_{16}),\\ W(\text{hex})_{m=\pm\frac{3}{2}}&=-(9/192)(eM_{16}m_{16}),\\ W(\text{hex})_{m=\pm\frac{5}{2}}&=(1/64)(eM_{16}m_{16}).\end{aligned}\quad (11)$$

Similarly, for $I=7/2$, the energy levels are:

$$\begin{aligned}W(\text{hex})_{m=\pm\frac{1}{2}}&=(9/448)(eM_{16}m_{16}),\\ W(\text{hex})_{m=\pm\frac{3}{2}}&=-(3/448)(eM_{16}m_{16}),\\ W(\text{hex})_{m=\pm\frac{5}{2}}&=-(13/448)(eM_{16}m_{16}),\\ W(\text{hex})_{m=\pm 7/2}&=(1/64)(eM_{16}m_{16}).\end{aligned}\quad (12)$$

III. APPARATUS

A. General Considerations

Requirements for a good spectrometer include wide frequency coverage, high sensitivity, and low distortion. Since the resonance frequencies of direct nuclear quadrupole transitions are molecular or atomic properties and there are no laboratory means available for simulating these tremendous fields, the radio-frequency oscillator of the spectrometer should be capable of

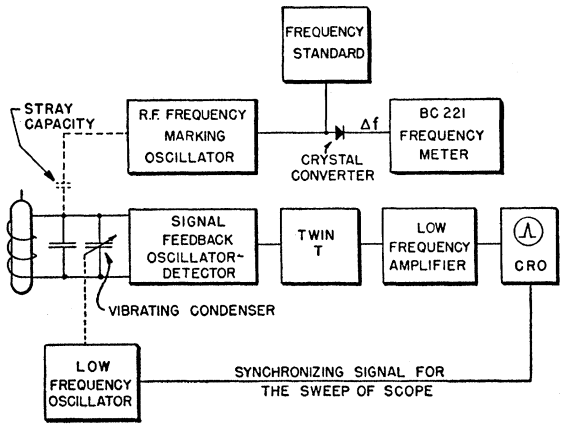

FIG. 4. Block diagram of rf spectrometer for pure nuclear quadrupole resonances.

tuning over a wide frequency range in order to cover the frequencies of quadrupole resonances. To detect the very weak signal of the pure nuclear quadrupole resonance, a spectrometer of high sensitivity is required. Accurate measurements also require that the electronic system incorporated in the spectrometer reproduce the shape of resonance lines accurately. In general the nuclear quadrupole interaction is characterized by a shorter relaxation time than the nuclear magnetic interaction; hence a greater rf field is needed to produce an observable resonance. Neither the Bloch cross-coil nor the Purcell bridge method are capable of giving adequate sensitivity for a pure nuclear quadrupole resonance experiment because of difficulty of balancing out the large primary rf signal which is used to induce the nuclear signal. An unbalanced circuit developed by Pound and Knight[20] would also be inadequate in this application as it operates well only at low rf levels. A super-regenerative system has the advantage of wide frequency coverage and high sensitivity, although it too has important shortcomings. The most important of these is the ambiguity which arises from the presence of spurious signals resulting from the production of sidebands separated by the quenching frequency. In addition, there is empirically observed dependence of line-shape and line width upon the frequency and amplitude of the quenching voltage.[11] A satisfactory circuit, which is called "Signal Feedback Oscillator-Detector" will be discussed later.

The block diagram of the whole system is shown in Fig. 4. The main part of this setup is similar to the system used by Livingston.[21] The crystalline sample is placed in the coil of the rf tank circuit of the oscillator-detector. When the rf oscillator is tuned to the neighborhood of the quadrupole resonance line, the frequency of the oscillator is swept to and fro across the quadrupole resoannces by a vibrating condenser.[22] Because of quadrupole resonance, a minute amount of energy is absorbed from the coil causing the effective Q of the coil to decrease by a small amount. This effect, in turn, will cause a small rf voltage drop across the tank circuit which can be detected by the detecting device in the oscillator. The signal feedback device gives additional amplification directly in the detection tube, and hence avoids possible difficulty due to noise introduced by a subsequent stage of amplification. At the same time it provides amplification over a narrow band width. The low-frequency amplifier[23] amplifies the signal and then delivers it to the verticle deflection system of the scope. The horizontal sweep of the scope is synchronized with the low-frequency oscillator which controls the vibrating condenser. Through this arrangement, the resonance line is displayed on the screen of the scope.

B. Signal Feedback Oscillator-Detector

The circuit arrangement of the signal feedback oscillator-detector is shown in Fig. 5. The 6AK5 tube acts simultaneously as an rf oscillator and a detector. The oscillator is essentially a split-resistance grounded-plate Colpitts circuit with feedback obtained by means of the stray capacitances while the detector is a combination of the grid-leak and plate types. The circuit has been used by Hopkins[24] and Livingston[21] but in their case the tube operates at a different point of its characteristic. The present arrangement has the advantage of only one "hot" lead to the rf tank circuit and avoids an extra detector which would otherwise connect to the tank with attendant decrease in Q. The excitation ratio for the oscillator is governed by the ratio of the "regeneration" resistor to the 1.5-megohm grid-leak. When the vibrating condenser sweeps the oscillator frequency across the nuclear resonance, a decrease in rf voltage due to absorption in the sample appears across the tank and will be detected at the

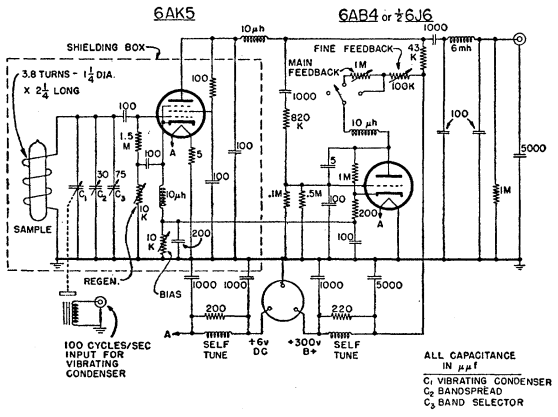

FIG. 5. Schematic diagram of signal feedback oscillator-detector.

[20] R. V. Pound and W. D. Knight, Rev. Sci. Instr. **21**, 219 (1950).
[21] R. Livingston, Ann. N. Y. Acad. Sci. **55**, 800 (1952).
[22] Part of surplus APN-1 Radio Altimeter.
[23] A. Hewlett Packard amplifier operates with a power amplification of 40 db.
[24] N. J. Hopkins, Rev. Sci. Instr. **20**, 401 (1949).

plate of the 6AK5 tube. This signal represents the absorption mode which results from the imaginary part of the nuclear susceptibility.

The mechanism of operation is shown graphically in Fig. 6. By adjusting the "bias" control potentiometer, the dc grid bias is set almost to the cut-off point. Due to the use of the cathode bias system, the cut-off action is extremely slow. The rf grid swing is adjusted to be slightly greater than the bias voltage (on the verge of "Class B_1" and "Class B_2" operation). At the rf peak, the grid is only very slightly positive ("Class B_2"). The circuit parameters are adjusted so as to use the steepest possible slope of the characteristic in order to have good detection. However, when a signal appears, because of grid rectification the bias is decreased slightly as shown in Fig. 6 and cancels out the detection action to some degree. The feedback arrangement counteracts this loss and reinforces the signal.

Another factor which increases the signal-to-noise ratio is the fact that the $R-C$ time constant (about 10^{-3} second) of the coupling network at the grid side of the 6J6 is adjusted to match the reciprocal of the width of the resonance line. Hence a frequency-selective characteristic for the circuit is incorporated within the feedback loop associated with the 6J6 tube. In this way, one can avoid the use of a high-gain narrow-band amplifier in the following stage. The rf level across the tank ranges from 5 to 13 volts. A specially designed high-μ tube which could operate at a high rf level might give more sensitive detection for a nuclear signal of shorter relaxation time. The detection characteristic for the 6AK5 with feedback is shown in Fig. 7.

It was found that Raytheon 5654 tubes were superior to ordinary 6AK5 tubes in this application. Good shielding between the rf and af (audio-frequency) circuits is absolutely essential for the operation of the feedback circuit. In the present apparatus, rf and af circuits are located in separate copper compartments and all feed-through connections are made with button condensers. The complete system is enclosed in a copper box. Two similar circuits were built, one to cover the range from 10–60 Mc/sec and the other from 60–120 Mc/sec.

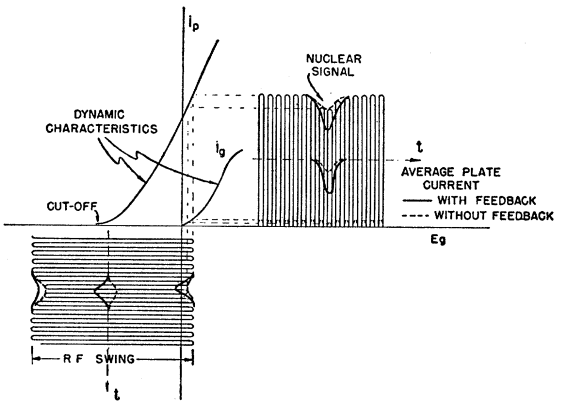

FIG. 6. Operating behavior of signal feedback oscillator-detector.

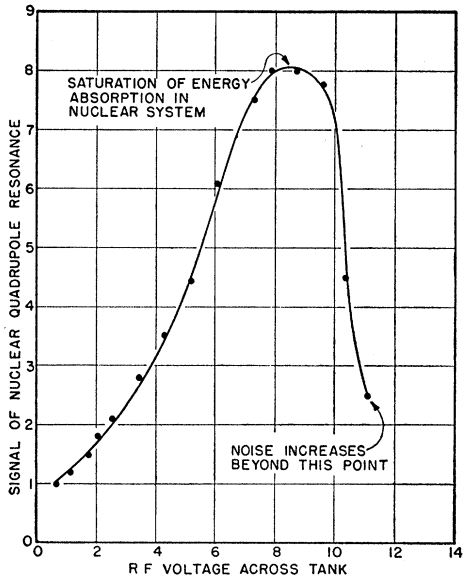

FIG. 7. Detection characteristic of 6AK5 used as signal feedback oscillator-detector (Cl^{35} in a single crystal of p-$C_6H_4Cl_2$ was used).

The signal of the Cl^{35} resonance in $NaClO_3$ at room temperature is shown in Fig. 8. The theoretical signal to noise ratio is about 20.

C. Frequency Measurement

A 100-kc/sec crystal oscillator which is stabilized to several parts in 10^7 with respect to WWV, serves as the frequency standard. By frequency multiplication, harmonics at 5, 20, and 40 Mc/sec are available as references for accurate frequency measurements. Usually the 5 and 20 Mc/sec standard signals are applied together to a 1N34 crystal which serves as mixer and harmonic generator simultaneously. Thus, frequency markers at 5-Mc/sec intervals are available from 5 Mc/sec up to several hundred Mc/sec. A frequency-marking oscillator which interacts with the frequency-modulated oscillator-detector will produce a characteristic pip on the scope. If this pip is placed on the center of the absorption line, the resonance frequency can be determined with a BC-221 frequency meter which measures the beat frequency Δf between the marking oscillator and the nearest frequency marker from the standard. In this way, the absolute frequency can be determined within several hundred cycles, being limited only by the accuracy of the BC-221 meter. A TS-323 frequency meter is used as the marking oscillator and for rough frequency checks.Sometimes a Gertsch FM-3 frequency meter is good enough for the accurate frequency measurement in the region of the fundamental frequency of its searching oscillator. Since the frequency of the quadrupole resonance is sensitive to temperature, the sample temperature is kept constant within 0.1°C by a mercury contact thermostat.

TABLE I. Measurements of chlorine quadrupole resonances in different compounds.

Compound	Isotope	Temp. °C	Resonance freq. (Mc/sec)	Signal to noise	Half-intensity width (kc/sec)	Date of experiment
	Cl^{35}	27.4[a]	34.23324±0.00025	15	1.43	March 19, 1952
	Cl^{37}		26.97952±0.00025	5	1.40	
	Cl^{35}	16.9	34.29402±0.00025	12	1.38	March 17, 1952
Para-$C_6H_4Cl_2$	Cl^{37}		27.02771±0.00025	4	1.23	
(single crystal)	Cl^{35}	0.3	34.34609±0.00025	12		March 20, 1952
	Cl^{37}		27.06887±0.00025	4		
	Cl^{35}	−195	34.77540±0.00025	19	2.74	March 25, 1952
	Cl^{37}		27.40811±0.00025	4		
	strong lines Cl^{35}	25.5	19.17496±0.00050	10	2.28	April 1, 1952
	strong lines Cl^{37}		15.11125±0.00025	3		
	strong lines Cl^{35}	0.6	19.19916±0.00050	10	2.92	Feb. 26, 1952
	strong lines Cl^{37}		15.13058±0.00025	3		
	strong lines Cl^{35}	−195	19.30468±0.00050	12	3.56	March 28, 1952
$SbCl_3$	strong lines Cl^{37}		15.21522±0.00025	4		
(polycrystal)	weak lines Cl^{35}	25.5	20.40739±0.00050	4		April 1, 1952
	weak lines Cl^{37}		16.08146±0.00025	1.5		
	weak lines Cl^{35}	0.6	20.47433±0.00050	4		Feb. 26, 1952
	weak lines Cl^{37}		16.13457±0.00025	1.5		
	weak lines Cl^{35}	−195	20.90767±0.00050	4		March 28, 1952
	weak lines Cl^{37}		16.47790±0.00025	2		
	p.c.[b] Cl^{35}	23.8	29.92864±0.00050	9	0.57	July 25, 1952
	p.c.[b] Cl^{37}		23.58894±0.00025	3	0.52	
$NaClO_3$	s.c.[b] Cl^{35}	0.4	30.02468±0.00050	15	1.35	March 7, 1952
	s.c.[b] Cl^{37}		23.66998±0.00025	4	1.13	
	p.c. Cl^{35}	−195	30.63017±0.00025	20	1.87	July 9, 1953
	p.c. Cl^{37}		24.14228±0.00025	4	1.07	
CH_3Cl	Cl^{35}	−195	34.02341±0.00025	8	5.44	April 17, 1952
(polycrystal)	Cl^{37}		26.81552±0.00025	2		
	Cl^{35}	−195	35.9862±0.0008	8	2.6	Dec. 17, 1951
Trans-$C_2H_2Cl_2$	Cl^{37}		28.3646±0.0008	2		

[a] High-temperature phase (sample heated over 40°C, cooled again). See C. Dean and R. V. Pound, J. Chem. Phys. **20**, 195 (1952).
[b] p.c. = polycrystal; s.c. = single crystal.

IV. CHLORINE SPECTRUM

A. General Aspects

Both of the stable chlorine isotopes (Cl^{35}, Cl^{37}) have a nuclear spin of $\frac{3}{2}$. Each isotope, therefore, has only one pure nuclear quadrupole transition. Results of measurements of these transitions in various molecules at different temperatures are tabulated in Table I. In general, these data are taken at three temperature points (room temperature, temperature of melting ice, and liquid nitrogen temperature). Although no attempt was made to measure the absolute temperature accurately, the relative temperature at each measuring point was kept constant within 0.1°C. The temperature coefficient of nuclear quadrupole resonance frequencies and the ratio, $(eQq)_{Cl^{35}}/(eQq)_{Cl^{37}}$, in different compounds are listed in Table II.[25]

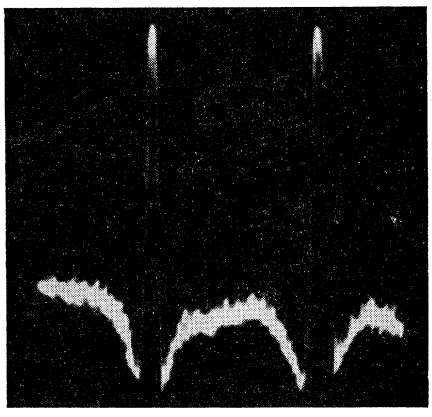

FIG. 8. Signal of pure quadrupole resonances of Cl^{35} in $NaClO_3$ at room temperature. (Double pips appear because of the vibrating condenser sweeping across the resonance frequency twice in one cycle.)

The ratio of the magnetic moment of Cl^{35} to that of Cl^{37} is 1.2 and the ratio of their abundances 75.4/24.6, hence, the expected ratio of signal intensities[26] is 4.2

[25] Some preliminary results were published in reference 4.

[26] If one uses the Pound formula (reference 6) with some modification, the signal-to-noise amplitude ratio will be

$$\frac{A_s}{A_n}=\frac{V_0^{\frac{1}{2}}Q_0^{\frac{1}{2}}\zeta^{\frac{1}{2}}\hbar^2\gamma N_0\sin\theta\nu_0^{\frac{3}{2}}T^{*\frac{1}{2}}(I+m)(I-m+1)}{32kT_c(2I+1)(2\pi kT_dBFT_1)^{\frac{1}{2}}}$$

for the pure quadrupole resonances, where θ is the angle between the rf field and q. The ratio of signal intensities for the two isotopes should be proportional to the ratio of natural abundances, the ratio of magnetic moments, the $\frac{3}{2}$ power of the ratio of eQq's, and to the square root of the ratio of the (T_2^*/T_1) values.

to 1. This value is in rough agreement with the experimental values given in Table I. From Table I one may note that the line width increases with a decrease of temperature (from room temperature to liquid nitrogen temperature). This effect might be attributed to an increase of strains in crystals as the temperature of the sample was reduced.

B. Temperature Dependence

It has been shown in Fig. 3 that eQq and therefore the quadrupole resonance frequency will, in general, decrease with an increase of temperature. The experimental negative temperature coefficients of the resonances lines support this prediction. For *para*-chlorobenzene, since the molecular torsional vibrations are well known, the value of the frequency coefficient of the resonances of Cl^{35} as given by Eq. (6) can be easily calculated. At 16.9°C the predicted value of the fractional change in frequency per degree change in temperature is -7.11×10^{-5} whereas the experimental one is -9.16×10^{-5}. Equation (7) also predicts that the ratio $(eQq)_{Cl^{35}}/(eQq)_{Cl^{37}}$, should decrease with a decrease of temperature. The data given in Table II also agrees with this predicted variation. For the case of *para*-dichlorobezene, the calculated change in ratio, $(eQq)_{Cl^{35}}/(eQq)_{Cl^{37}}$, is -2.2×10^{-5} for a decrease of temperature from 289.9°K to 78°K, whereas the measured change is $-(4.7\pm1)\times10^{-5}$. This agreement of theory with experiment indicates that the thermal vibrations proposed by Bayer do play a major role in the temperature dependence of nuclear quadrupole interactions.

In antimony trichloride there are two pairs of resonance frequencies (for Cl^{35} and Cl^{37}), which have different dependence on temperature. From this observation, one may conclude that there are two nonequivalent sites for the chlorine atoms in the crystal lattices. The exact structure of this crystal is as yet not known. For sodium chlorate, the temperature variation of the ratio $(eQq)_{Cl^{35}}/(eQq)_{Cl^{37}}$, shows the same trend as other compounds, but with a considerable smaller magnitude. This might be attributed to the fact that the chlorine atoms are situated near the mass center of molecules, so that the isotopic effect on torsional vibrations is small.

C. Nuclear Polarization

In the earlier measurements of $(eQq)_{Cl^{35}}/(eQq)_{Cl^{37}}$, discrepancies of about two percent were found for different molecular environments. In an attempt to explain this effect, a theory of nuclear polarization by surrounding electric field was suggested.[27] Actually some of the experimental data of earlier experiments contains errors whose magnitudes are comparable to the aforementioned discrepancies. The data of the present experiment, which have the probable error of about 0.001 percent, show that the variation of the ratio, $(eQq)_{Cl^{35}}/(eQq)_{Cl^{37}}$, is less than 0.024 percent and that it is dependent upon temperature as well as molecular environments (as shown in Table II). It has been pointed out in the last section that this variation of ratio, $(eQq)_{Cl^{35}}/(eQq)_{Cl^{37}}$, is to be attributed largely to molecular torsional vibrations. Moreover, the recent more accurate measurements of the ratio, $(eQq)_{Cl^{35}}/(eQq)_{Cl^{37}}$, in atomic chlorine by the atomic beam method (the ratio is 1.2686 ± 0.0004)[28] and in CH_3Cl (the ratio is 1.2685 ± 0.0002) and SiH_3Cl (the ratio is 1.2687 ± 0.0005) by the microwave absorption method[29] also supports the results of the present measurement. Therefore, it can be concluded that while nuclear polarization by electric field undoubtedly does exist, its effect on the present measured variations of ratio $(eQq)_{Cl^{35}}/(eQq)_{Cl^{37}}$ is largely masked by thermal vibrations.

D. Relaxation Time

In the present experiment, the spin lattice relaxation time T_1 is measured by the saturation of the rf field

TABLE II. Ratio $(eQq)_{Cl^{35}}/(eQq)_{Cl^{37}}$, and temperature coefficients of resonance lines of Cl in different compounds.

Compound	Isotope	Temp. °C	Temp. coef. of reson. freq. (kc/°C)	Ratio $\frac{(eQq)_{Cl^{35}}}{(eQq)_{Cl^{37}}}$
		27.4[a]		1.268860 ±0.00001
Para-$C_6H_4Cl_2$ (single crystal)	Cl^{35}	16.9	−3.14	1.268847
	Cl^{37}		−2.48	±0.00001
		0.3		1.268841 ±0.00001
	Cl^{35}		−2.20	1.268800
	Cl^{37}	−195	−1.74	±0.00001
$SbCl_3$ (polycrystal) strong lines	Cl^{35}	25.5	−0.972	1.268920
	Cl^{37}		−0.776	±0.00002
		0.6		1.268898 ±0.00002
	Cl^{35}		−0.54	1.268774
	Cl^{37}	−195	−0.43	±0.00002
$SbCl_3$ (polycrystal) weak lines	Cl^{35}	25.5	−2.69	1.269001
	Cl^{37}		−2.13	±0.00002
		0.6		1.268973 ±0.00002
	Cl^{35}		−2.22	1.268831
	Cl^{37}	−195	−1.76	±0.00002
$NaClO_3$ p.c.[b]	Cl^{35}	23.8	−4.10	1.268757
	Cl^{37}		−3.25	±0.00002
$NaClO_3$ s.c.[b]		0.4		1.268739 ±0.00002
$NaClO_3$ p.c.	Cl^{35}	−195	−3.10	1.268736
	Cl^{37}		−2.44	±0.00001
CH_3Cl (polycrystal)		−195		1.268795 ±0.00001
Trans-$C_2H_2Cl_2$		−195		1.26870 ±0.00006

[a] High-temperature phase.
[b] p.c. ≡ polycrystal; s.c. ≡ single crystal.

[27] Gunther-Mohr, Geschwind, and Townes, Phys. Rev. **81**, 289 (1951).

[28] V. Jaccarino and J. G. King, Phys. Rev. **83**, 471 (1951).

[29] R. L. White (private communication).

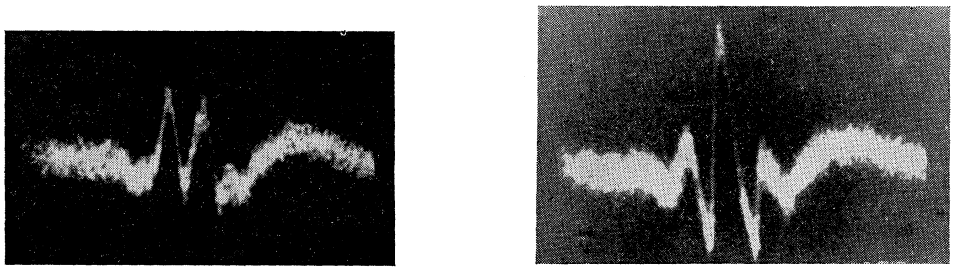

(a) (b)

FIG. 9. Zeeman splittings of pure quadrupole resonance line of Cl^{35} in a single crystal of $NaClO_3$. (a) and (b) indicate different orientation of magnetic field with the crystal.

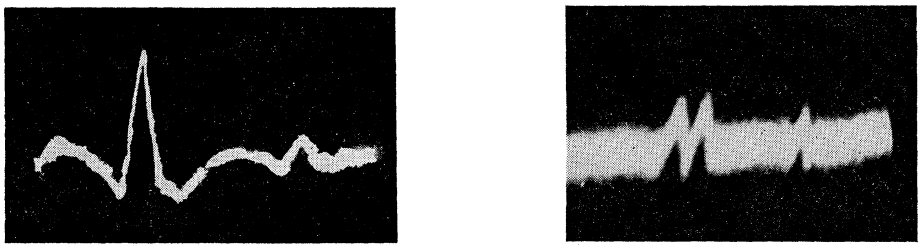

(a) (b)

FIG. 10. Resonance lines of Cl^{35} arising from coexistence of two different phases in a single crystal of p-$C_6H_4Cl_2$. (a) Resonance lines. (b) Zeeman splitting.

and the apparent transverse relaxation time T_2^* by the width of the resonance at half-maximum intensity. Results of measurements of these values at room temperature are given in Table III. The measurement of T_1 and T_2^* in $NaClO_3$ is in agreement with the results obtained from a measurements by the free-induction method.[30] The crystal structure of $NaClO_3$ was determined by Zachariasen.[31] This crystal has cubic structure with a unit cell 6.555 A on a side, containing four molemolecules. The Na—Cl distance given by Zachariasen's molecular structure is 1.59 A. However, from the position parameters of sodium and chlorine nuclei in the unit cell as given by the same author, this distance can be evaluated as 4.01 A. It is more likely that the latter value is correct, since the former gives too high a magnetic field at the chlorine nucleus due to the sodium nucleus.

E. Crystal Structure and Zeeman Effect

By introducing a weak magnetic field in the single crystal sample of sodium chlorate, Zeeman splittings of the resonance line of Cl^{35} were observed as shown in Fig. 9(a) and (b). These patterns are different for different orientation of the magnetic field within the crystal. Two Cl^{35} lines in Fig. 10(a) are due to the coexistence of the two phases of *para*-dichlorobenzene. This phenomenon occurs when a single crystal is heated above 40°C and then gradually cooled to room temperature. The interval between these two Cl^{35} lines as shown in Fig. (10a) is about 20 kc/sec. Figure 10(b) shows the difference of Zeeman splitting patterns of two different resonance lines. These differences indicate that the molecules of *para*-$C_6H_4Cl_2$ are oriented differently in the different phases of the crystal.

TABLE III. Measurements of relaxation time T_1 and T_2^*.

Compound	Isotope	T_1 seconds	T_2^* milliseconds
$NaClO_3$	Cl^{35}	0.039	0.56
	Cl^{37}	0.028	0.61
p-$C_6H_4Cl_2$	Cl^{35}	0.022	0.23

[30] E. L. Hahn and B. Herzog, Phys. Rev. **93**, 639 (1954).
[31] W. H. Zachariasen, Z. Krist. **71**, 517 (1929).

V. ANTIMONY SPECTRUM

A. General Discussion

Sb^{121} possesses a spin of 5/2 and Sb^{123} a spin of 7/2, therefore Sb^{121} has two pure quadrupole resonance transitions and Sb^{123} has three.[32] Results of measurements are tabulated in Table IV. Each set of five transitions in one compound was measured at a temperature which was held constant to within 0.1°C. Two sets of data were taken for each molecule at different temperature points. In the last column in Table IV, ν_3^{123}(calc) are values of ν_3^{123} as calculated from measured values of ν_1^{123} and ν_2^{123} from Eq. (4), while ν_3^{123}(meas'd) are experimental values. The $(eQq)_{Sb^{123}}/(eQq)_{Sb^{121}}$ ratio

[32] Pure quadrupole resonances of antimony isotopes in $SbCl_3$ were first observed by H. G. Dehmelt and H. Krüger, see Z. Physik **130**, 385 (1951).

TABLE IV. Measurements of antimony quadrupole resonances in different compounds.

Compound	Temp. °C	Isotope	Transition	Signal to noise	Resonance freq. (Mc/sec)	Half-intensity width (kc/sec)	eQq (Mc/sec)	Remarks (values in Mc/sec)	Date of experiment
$SbCl_3$ (single crystal)	31.07	Sb^{121}	ν_1^{121}	5:1	58.07831	5.18	376.90239	ν_3^{123}(calc)=102.69226	Aug. 13, 1952
			ν_2^{121}	3:1	112.49849	8.07			
		Sb^{123}	ν_1^{123}	5:1	37.33261	5.32	480.45424	ν_3^{123}(meas'd)=102.69037	
			ν_2^{123}	3:1	67.72563				
	0.8	Sb^{121}	ν_1^{121}	5:1	58.37421	7.08	378.27006	ν_3^{123}(calc)=103.05003	Sept. 13, 1952
			ν_2^{121}	3:1	112.87532	5.53			
		Sb^{123}	ν_1^{123}	5:1	37.62624	6.13	482.19602	ν_3^{123}(meas'd)=103.04629	
			ν_2^{123}	3:1	67.92500				
$SbBr_3$ (single crystal)	31.04	Sb^{121}	ν_1^{121}	5:1	48.35638	9.23	320.01353	ν_3^{123}(calc)=87.35376	Nov. 6, 1952
			ν_2^{121}	5:1	95.87212	14.00			
		Sb^{123}	ν_1^{123}	3:1	29.84304	11.15	407.92664	ν_3^{123}(meas'd)=87.35369	
			ν_2^{123}	3:1	58.05708				
	0.4	Sb^{121}	ν_1^{121}	5:1	48.65959	14.32	321.92938	ν_3^{123}(calc)=87.87824	Nov. 28, 1952
			ν_2^{121}	5:1	96.44099	10.14			
		Sb^{123}	ν_1^{123}	3:1	30.04807	12.29	410.38583	ν_3^{123}(meas'd)=87.87624	
			ν_2^{123}	3:1	58.39938	11.53			
Sb_2S_3 (single crystal)	30.75	Sb^{121}	ν_1^{121}	3:1	44.33480	9.89	295.54679	ν_3^{123}(calc)=80.72903	June 5, 1953
			ν_2^{121}	3:1	88.66300				
		Sb^{123}	ν_1^{123}	3:1	26.91568		376.73771	ν_3^{123}(meas'd)=80.72829	
			ν_2^{123}	2:1	53.81785				
	0.2	Sb^{121}	ν_1^{121}	5:1	44.80731	11.16	298.69326	ν_3^{123}(calc)=81.59109	June 24, 1953
			ν_2^{121}	3:1	89.60674				
		Sb^{123}	ν_1^{123}	3:1	27.20256		380.70651	ν_3^{123}(meas'd)=81.58955	
			ν_2^{123}	2:1	54.39268				

and the field asymmetry parameter η are given in Table V.

In general, signals of these antimony resonances are found to be much weaker than those of chlorine resonances. In order to cover the required frequency range, different coils were used and the signal to noise ratio for each line is given in Table IV. Observations of ν_1^{121} and ν_2^{123} were made with the same rf coil. The ratio of natural abundances of Sb^{121} and Sb^{123} is 56/44 and the ratio of their magnetic moments (3.3595)/(2.5470); therefore the theoretical estimated ratio of signal intensities between ν_1^{121} and ν_2^{123} is about 5:3. This value is in good agreement with the experimental values in Table IV. All line widths of the antimony resonances are considerably greater than those of the chlorine resonances. The probable explanation for this broadness lies in the fact that the stronger quadrupole interaction of antimony nuclei shortens the relaxation time.

Single crystals of $SbCl_3$ and $SbBr_3$ used in this experiment were grown in the laboratory, whereas the single crystals of Stibnite (Sb_2S_3) were natural ones.

B. Quadrupole Coupling Constants and Ratios

The temperature dependence of the quadrupole coupling constants of antimony has the same tendencies as those of chlorine; namely an increase of temperature is associated with a decrease of quadrupole coupling constants as shown in Table IV. In Table V, one may note that the ratio, $(eQq)_{Sb^{123}}/(eQq)_{Sb^{121}}$, varies only by 0.005 percent with temperature and with different molecular environments. This small change in the ratio of (eQq) between two antimony isotopes may be attributed to the greater mass of antimony which makes them less sensitive to thermal vibrations. The lack of

TABLE V. Ratio of eQq's and asymmetry parameter, η, of antimony isotopes in different compounds.

Compound	Temp. °C	Isotope	η, asymmetry parameter	Ratio $\frac{(eQq)_{123}}{(eQq)_{121}}$
$SbCl_3$ (single crystal)	31.07	Sb^{121}	±0.15919	1.274744
		Sb^{123}	±0.15923	±0.00001
	0.8	Sb^{121}	±0.16357	1.274740
		Sb^{123}	±0.16354	±0.00001
$SbBr_3$ (single crystal)	31.04	Sb^{121}	±0.08236	1.274717
		Sb^{123}	±0.08217	±0.00001
	0.4	Sb^{121}	±0.08393	1.274770
		Sb^{123}	±0.08363	±0.00001
Sb_2S_3 (single crystal)	30.75	Sb^{121}	±0.0076	1.274714
		Sb^{123}	±0.0077	±0.00001
	10.2	Sb^{121}	±0.0082	1.274754
		Sb^{123}	±0.0073	±0.00002

variation in the coupling ratio $(eQq)_{Sb^{123}}/(eQq)_{Sb^{121}}$ affords no evidence of nuclear polarization for those nuclei. The temperature dependence of this ratio has the same sign as that for the chlorine isotopes, that is the ratio of eQq of the lighter isotope to that of the heavier isotope decreases with a decrease of temperature. The only exception was in the case of $SbCl_3$, in which the ratio, $(eQq)_{Sb^{123}}/(eQq)_{Sb^{121}}$, was found to be constant to within four parts in one million. This variation is less than the probable experimental error.

C. Field Asymmetry Parameter

Values of the field asymmetry parameter, η, as obtained from measurements are shown in Table V. The spins of Sb^{121} and Sb^{123} are different, consequently their energy levels are different. Measurements show that η^{121} and η^{123} agree exceedingly well, especially for $SbCl_3$ which indicates the high consistency of the experimental data. However, a small disagreement (in general less than 0.3 percent in magnitude of η) exists between η^{121} and η^{123}. This difference may be due to the isotopic effect on the thermal vibrations. Moreover, one may note in Table V, that values of η for both isotopes change with temperature as might be expected from effects of thermal vibrations. The frequency, ν_3^{123}, calculated from η_{123} and $(eQq)_{Sb^{123}}$ which are obtained from ν_1^{123} and ν_2^{123} by Eq. (4), shows a disagreement of only several parts in one hundred thousand with the measured ν_3^{123}. The errors (which are evaluated from experimental errors in ν_1^{123} and ν_2^{123}) in ν_3^{123} as calculated by Eq. (4) is less than one kc/sec, and the error of the measured frequency ν_3^{123} is even smaller (about 300 cps). This discrepancy is, in general, two or three times larger than is to be expected. A possible explanation will be given in the next section.

D. Effect of Hexadecapole Interactions

The discrepancy pointed out in the last section is very interesting. It cannot be due to polarization of the nucleus by surrounding electronic charges, since Gunther-Mohr, Geschwind, and Townes[27] have shown that the energy connected with nuclear polarization depends on angle in the same way as that due to quadrupole interactions.

It was shown above (Sec. II-D), that the ratio between the magnitudes of the electric hexadecapole coupling constant and the electric quadrupole coupling constant for an atom is of the order of r_n^2/r_{eff}^2. In the present case, r_n^2, as determined either from the magnitude of their quadrupole moments or from the well-known formula for nuclear radii is about 10^{-24} cm^2 for the antimony isotopes. The valence electrons of antimony are in a $5p$-orbital which may be hybridized with $5d$-orbitals. The $5d$-electrons will be responsible for the hexadecapole field m_{16}. A simple calculation using hydrogenic wave functions shows that $1/r_{\text{eff}}^2 > (1/10^{-19})$ cm^{-2} for a Sb $5d$-electron. Therefore, the ratio $(eM_{16}m_{16})/eQq$ is about 10^{-5} for antimony isotopes. This is the same order of magnitude as the discrepancy mentioned above.

The set of data on the quadrupole resonances in $SbBr_3$ at 0.4°C was taken with a great deal of care. By using Eq. (4) and Eq. (12), the constants of Sb^{123} can be evaluated as

$$|(eQq)_{Sb^{123}}| = 410.3814 \text{ Mc/sec},$$
$$\eta^{123} = \pm 0.0836145,$$
$$|(eM_{16}m_{16})_{Sb^{123}}| = 24.0 \pm 5 \text{ kc/sec}.$$

The results of the calculation indicates that $(eM_{16}m_{16})_{Sb^{123}}$ is opposite in sign to $(eQq)_{Sb^{123}}$. The ratio $(eM_{16}m_{16})_{Sb^{123}}/(eQq)_{Sb^{123}}$ is about 10^{-5} which agrees fairly well with the theoretical estimate given above.

One may assume that the asymmetry parameter η for Sb^{121} is 0.0836145, the same as for Sb^{123} at the same temperature. Substituting this η and the measured values of ν_1^{121} and ν_2^{121} given in Table IV into Eq. (3) and Eq. (11) and solving for $(eQq)_{Sb^{121}}$ and $(eM_{16}m_{16})_{Sb^{121}}$, one obtains

$$|eQq_{Sb^{121}}| = 321.93223 \text{ Mc/sec},$$
$$|(eM_{16}m_{16})_{Sb^{121}}| = 30.3 \pm 5 \text{ kc/sec}.$$

As in the case of Sb^{123}, $(eM_{16}m_{16})_{Sb^{121}}$ and $(eQq)_{Sb^{121}}$ are opposite in sign. Similarly, the ratio $(eM_{16}m_{16})_{Sb^{121}}/(eQq)_{Sb^{121}}$ is of the order of 10^{-5}. Furthermore, by taking the ratio, one obtains:

$$\frac{(eQq)_{Sb^{123}}}{(eQq)_{Sb^{121}}} = 1.274745 \pm 0.00001,$$
$$\frac{(eM_{16}m_{16})_{Sb^{123}}}{(eM_{16}m_{16})_{Sb^{121}}} = 0.8 \pm 0.3.$$

One might think that the discrepancy pointed out in Sec. V-C, arose from second order perturbations due to the nuclear quadrupole interaction with the valence electrons or with thermal vibrations. However, simple calculations will show that these effects are too small to explain the present discrepancy.

The second order perturbation of electronic states by the quadrupole interaction will give the energy shift

$$\Delta W_e = -\sum_{n'l'm'} \frac{(eQq_{n'l'm'nlm})(eQq_{n'l'm'nlm})}{E_{n'l'm'} - E_{nlm}},$$

where n', l', m' and n, l, m are quantum numbers which signify different electronic states of energy $E_{n'l'm'}$ and E_{nlm}. It has been pointed out by Townes[1] that $q_{n'l'm'nlm}$ are zero unless $m=m'$, $l=l'\mp 0$ or $l=l'\pm 2$. A good approximation is that $q_{n'l'm'nlm}$ is about one tenth of q (q_{nlmnlm}) for p-electrons and $eQq/(E_{n'l'm'}-E_{nlm})$ is about 10^{-6}, so that ΔW_e will be 10^{-8} eQq.

The effect of second-order perturbation of thermal vibrations by the quadrupole interaction can be cal-

culated by assuming simple harmonic vibrations, with the Hamiltonian

$$H_{\text{vib}}=\frac{P_\theta^2}{2I_\theta}+\frac{K\theta^2}{2},$$

where P_θ is the angular momentum, θ the angular amplitude of the vibration, I_θ the moment of inertia around the angular vibration axis, and K the torsional force constant. Hence, the vibration frequency will be $\omega_\tau=(K/I_\theta)^{\frac{1}{2}}$. The perturbation energy due to the quadrupole interaction is

$$H_Q'=\tfrac{1}{4}eQq(3\cos^2\theta'-1),$$

where $\theta'=\theta_I+\theta$, and θ_I is the angle between nuclear spin and the axis of symmetry of the electric gradient q. By the addition theorem for Legendre polynomials and using $\sin^2\theta\simeq\theta^2$ (for small θ), the perturbing Hamiltonian becomes

$$H_Q'=\tfrac{1}{4}eQq(3\cos^2\theta_I-1)(1-\tfrac{3}{2}\langle\theta^2\rangle_{\text{Av}}),$$

where $\langle\theta^2\rangle_{\text{Av}}$ indicates the average value of θ^2 under thermal vibrations.

Using the quantum-mechanical matrix elements for a simple harmonic oscillator, one obtains the first-order perturbation energy as,

$$\Delta W_1=-\tfrac{3}{8}eQq(3\cos^2\theta_I-1)(n+\tfrac{1}{2})\hbar/(I_\theta K)^{\frac{1}{2}},$$

where n is the vibration quantum number. The effect of this term is linear in $(3\cos^2\theta_I-1)$, so it will not change the interval rule of the nuclear quadrupole energy levels. This result is in agreement with Eq. (5).

The energy term due to the second-order perturbation is

$$\Delta W_2=\frac{9}{256}(eQq)^2(3\cos^2\theta_I-1)^2\frac{(2n+1)\hbar}{\omega_\tau I_\theta K}.$$

This energy depends on $(3\cos^2\theta_I-1)^2$, so it will give rise to a pseudo-hexadecapole effect. Taking $n=1$ for the first excited state, one obtains

$$\Delta W_2=\frac{27}{256}(eQq)(3\cos^2\theta_I-1)^2\frac{eQq}{\omega_\tau}\frac{\hbar}{I_\theta K}.$$

Substituting the appropriate molecular constants in the foregoing equation and simplifying, one obtains

$$\Delta W_2/h=5\times10^{-9}(eQq/h)(3\cos^2\theta_I-1)^2.$$

E. The Relation of Quadrupole Resonance to the Crystal Structure of Anitmony Compounds

The structure of stibnite, Sb_2S_3, has been determined.[33] It is known that the crystal forms a prolonged chain of indefinite length in a direction parallel the surfaces of cleavage. Each antimony atom is bonded to three sulfur atoms in a plane parallel to the chain axis. There are auxilliary Sb—S bonds existing in the crystal, which do not contribute considerably to the eQq of antimony. It is obvious that the field gradient q's for antimony atoms are in directions perpendicular to the chain axis. When the crystals were placed with their chain axis parallel to the rf coil axis (direction of the rf magnetic field), signals of pure quadrupole resonances due to antimony were observed with fairly good intensity. After the crystals were reorientated, with the chain axis perpendicular to the rf field, the signal disappeared. This behavior is to be expected from a theoretical consideration which shows that the signal intensity should vary with the sine of the angle between the rf field and the field gradient q.

Stibnite melts at 550°C. Crystals were heated to 450°C in an oven, then left there to anneal. When these annealed crystals were used as samples, the signal intensity was doubled. This effect indicates that the stibnite crystals were under some tension which was removed by annealing. When this is done, the field gradient q becomes more uniform and the signal strength is increased.

The very large asymmetry parameter η found in $SbCl_3$ and $SbBr_3$ indicates some type of intermolecular bonding in these crystals as has been shown to occur in I_2.[2] The two different sets of Cl resonances in $SbCl_3$ are probably also connected with intermolecular bonds.

ACKNOWLEDGMENTS

The author would like to thank Dr. V. W. Cohen of Brookhaven National Laboratory for the loan of the TS-323 frequency meter used as a marking oscillator. He also wishes to express his gratitude to Professor C. H. Townes for his guidance and encouragement during the experiment.

[33] W. Hofmann, Z. Krist. **86**, 225 (1933).

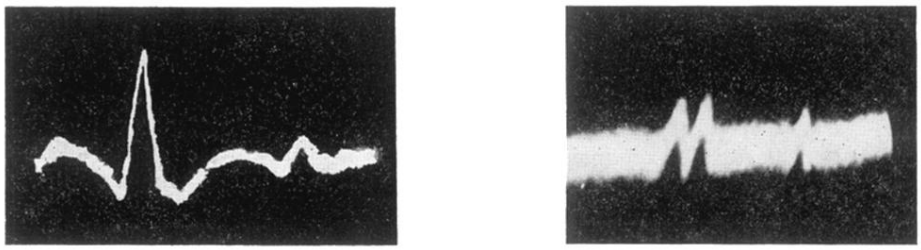

(a) (b)

FIG. 10. Resonance lines of Cl^{35} arising from coexistence of two different phases in a single crystal of p-$C_6H_4Cl_2$. (a) Resonance lines. (b) Zeeman splitting.

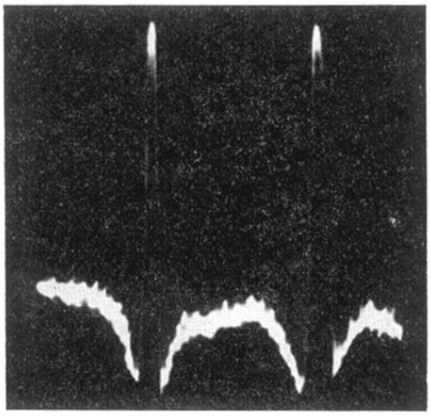

FIG. 8. Signal of pure quadrupole resonances of Cl^{35} in $NaClO_3$ at room temperature. (Double pips appear because of the vibrating condenser sweeping across the resonance frequency twice in one cycle.)

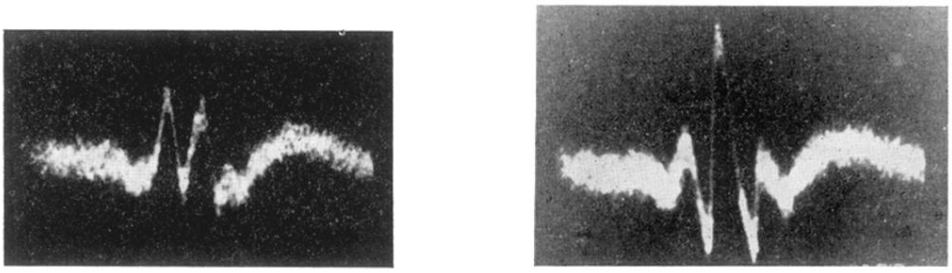

(a) (b)

FIG. 9. Zeeman splittings of pure quadrupole resonance line of Cl^{35} in a single crystal of $NaClO_3$. (a) and (b) indicate different orientation of magnetic field with the crystal.